Proceedings of the Mustansiriyah International Conference on Applied Physics (MICAP-2021)

Laser Intensity and Matrix Effect on Plasma Parameters for CuZn, Cu, and Zn Produced by Nd:YAG Laser

Raghad S. Mohammed[a,*], Kadhim A. Aadim[b] and Khalid A. Ahmed[a]

[a] *Department of Physics, College of Science, Mustansiriyah University, Palestine St., 10052, Baghdad, Iraq*
[b] *Department of Physics, College of Science, University of Baghdad, Baghdad, Iraq*

Doi: 10.12693/APhysPolA.140.306 *e-mail: raghad.almaliki@uomustansiriyah.edu.iq

The present work studies the relation of laser irradiance and matrix effect on plasma features of the CuZn, Cu, and Zn matrix. These matrices were irradiated by a Q-switched nanosecond Nd:YAG laser with the second harmonic wavelength (532 nm), and irradiance ranging from 2.1–4.8 $\times 10^8$ W/cm^2 at atmospheric pressure. The plasma parameters (T_e and n_e) were calculated by the Boltzmann plot and the Stark broadening methods. The results clarify no linear change in electron temperature at increasing laser irradiance for Cu and Zn plasma, except for the CuZn plasma. These fluctuations of electron temperature in those matrices are due to matrix effects. In contrast, the broadening of the line profiles related to electron density was evident with laser irradiance growth, causing an increase in electron density.

topics: laser intensity, matrix effect, plasma parameters

1. Introduction

Since the invention of the laser in 1960, laser-induced breakdown spectroscopy (LIBS) has been developed as an analytical technique. In this technique, plasma is produced by focusing a laser beam on the surface of a target and expands as a vapor plume. LIBS is called "microemission spectroscopy", it depends on atomic emission spectroscopy to analyze the material elemental composition [1–3]. The nature of laser-produced plasma depends on various factors, including laser intensity, wavelength, and the material chemical composition. Researchers have investigated the effect of these factors and the matrix effect on plasma production and its parameters [2].

The term "matrix effect" refers to the matrix dependence of analytical signal [4]. Matrix effects may be due to spectral, physical, and chemical effects. When strong lines of matrix element interfere with weak lines of analyzed element, the spectral matrix effect occurs. The physical matrix effect is related to variations in sample physical properties such as absorption coefficient, thermal conductivity, and the heat of vaporization, which impact the transfer of the ablated mass into plasma. The chemical matrix effect happens when the ionization tendency and the compound structure form product influences the emission characteristics of the analyte element [3, 5, 6]. Some previous studies were carried out to investigate the physical matrix effect on plasma parameters generated from binary samples. Sattar et al. [2] studied matrix effect on the spectroscopy of the Ag–Zn plasma in various concentrations ratios. This study aims to investigate laser intensity and matrix effects on plasma emissions and the characterization of CuZn, Cu, and Zn plasmas.

2. Materials and methods

In this experiment, plasma is generated utilizing nanosecond Q-switched Nd:YAG laser at the second harmonic wavelength (532 nm) with 10 ns pulse duration, 6 Hz repetition frequency, and laser irradiance ranging from 2.1–4.8$\times 10^8$ W/cm^2. Three samples were used, i.e., CuZn, Cu, and Zn. The purities of the targets were 99.98% — copper (Cu nanoparticle), 99.9999% — zinc (Zn nanoparticle). The Cu and Zn powders were mixed in specified proportions (0.5–0.953 wt% of Cu and 0.5–1.04 wt% of Zn) to form the CuZn matrix as a binary compound. These powders were pressed in a pellet form by applying 80 MPa pressure using a hydraulic press for 10 min. The laser beam was focused on the target surface at atmospheric pressure, utilizing a quartz lens with a 10 cm focal length. Optical fiber with a 50 μm diameter core collected the laser-produced plasma light from the CuZn, Cu, and Zn target surfaces.

The fiber was placed at 1 cm above the plasma, and was connected with the Surwit (S3000-UV-NIR) spectrometer to analyze the plasma emissions. To estimate the plasma characteristics the optical emission lines were assigned to of certain elements using NIST database software [7].

3. Results and discussion

3.1. Study of the spectral emission

The spectrum was recognized through ionic and atomic spectral lines emitted from plasma produced by laser with 532 nm wavelength. The emission spectra of CuZn, Cu, and Zn plasma covered the spectral range from 550 to 750 nm for CuZn and Cu and from 600 to 800 nm for Zn, as shown in Figs. 1–3, respectively. Figure 1 demonstrates that the emission spectrum of CuZn plasma consists of 11 lines, including 8 isolated lines for Cu II, Cu I, Zn I, Zn II, and 2 overlapping lines for Cu II and Zn II at 589 nm.

Figure 2 shows the Cu plasma spectrum, including 7 spectral lines, i.e, 5 lines for Cu II and 2 lines for Cu I. While the spectrum of Zn plasma consisted of 8 lines, as shown in Fig. 3, it includes 5 lines of Zn II and 3 lines of Zn I. The difference in emission lines may be attributed to differences in thermal and optical properties of CuZn, Cu, and Zn. These changes significantly influence the accuracy of quantitative estimations of LIBS in the emission intensity of copper and zinc elements in the three matrices due to physical properties or sample composition variations. The physical matrix effect caused these changes, which were related to the fact that the physical properties of the sample could change the ablation parameters. Although the concentrations of Cu and Zn in the mixed matrix were the same, these variations changed the quantity of ablated mass, resulting in differences in emission intensity.

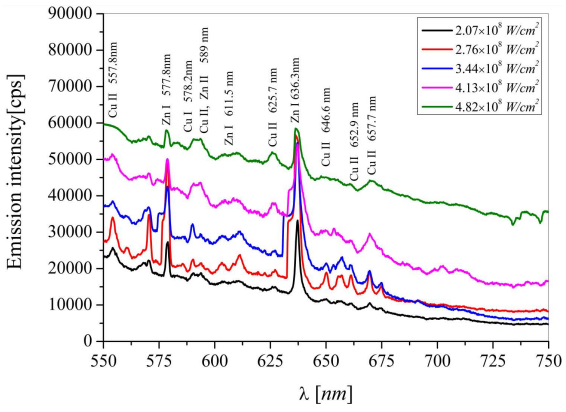

Fig. 1. Emission spectrum of CuZn plasma induced by 532 nm laser at different laser intensity.

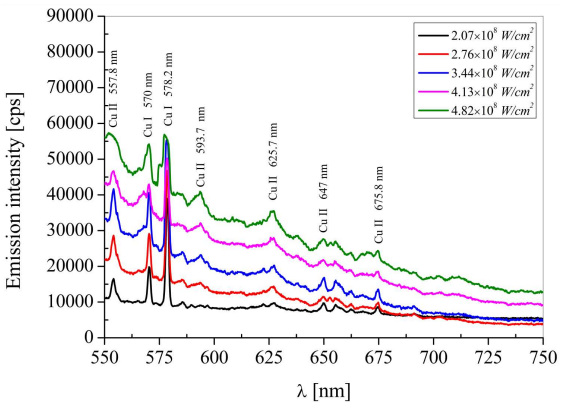

Fig. 2. Description as in Fig. 1, but for Cu plasma.

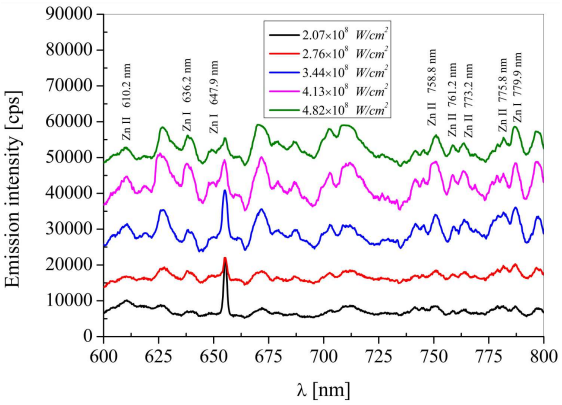

Fig. 3. Description as in Fig. 1, but for Zn plasma.

In contrast, these changes were also related to chemical matrix effects. This effect occurs when the emission features of one element are altered by the presence of another one [8]. In this study, the spectral matrix effects can be neglected. Spectral matrix effects can be avoided or minimized by using high-resolution spectrometers in LIBS (it enables the detection and elimination of some spectral interferences) and careful peak selection and/or selecting lines that do not exhibit spectral interference [9].

The spectrum was recorded at laser intensity ranging from 2.1 to 4.8×10^8 W/cm^2. We found that the LIPS signal intensity increases with laser intensity. The absorption of laser light by the plasma increases with increasing laser intensity, resulting in a rise in the ablation rate and increased spectral lines intensity. The increased intensity of plasma with rising laser intensity agrees with the previous study [10].

3.2. Plasma parameters

The spectral lines emitted from CuZn, Cu, and Zn plasma are helpful to estimate the essential plasma parameters, like electron temperature and electron density, T_e and N_e, respectively. They are the key parameters to understand the excitation and atomic ionization processes in plasma.

TABLE I

Data analysis from the Boltzmann plots with the linear fitting of R^2 and electron temperature at different laser intensity.

Laser intensity	CuZn matrix			Cu matrix			Zn matrix		
$\times 10^8$ [W/cm^2]	Slope	T_e [K]	R^2	Slope	T_e [K]	R^2	Slope	T_e [K]	R^2
2.07	−1.069	10847	0.992	−2.925	3966	0.998	−3.23	3591	0.888
2.76	−1.03	11262	0.983	−1.716	6759	0.894	−4.042	2870	0.925
3.44	−0.984	11795	0.967	−1.517	7646	0.829	−3.9731	2920	0.923
4.13	−0.793	14627	0.553	−1.894	6124	0.965	−3.910	2967	0.908
4.82	−0.787	14739	0.523	−1.963	5908	0.986	−3.927	2954	0.915

3.2.1. Electron temperature

Assuming that the local thermodynamic equilibrium (LTE) exists, the electron temperature of the CuZn, Cu, and Zn plasma are calculated using the Boltzmann plot method [11]

$$\ln\left(\frac{\lambda_{ji} I_{ji}}{g_j A_{ji}}\right) = -\frac{E_j}{k_B T} + C, \quad (1)$$

where the wavelength (λ_{ji}), statistical weight (g_i), probability of transition (A_{ji}), and upper energy (E_j) are obtained from the standard spectrum of NIST database [7], and i and j refer to the low and upper level, respectively. The Boltzmann constant is k_B, T is the plasma temperature, and C is a constant. Applying the Boltzmann plot method, we used three ionic lines (Cu II) at 625.7, 646.6, 652.9 nm for the CuZn plasma, and at 593.7, 625.7, 675.8 nm for the Cu plasma, also using ionic lines (Zn II) at 610.2, 761.2, 775.79 nm for the Zn plasma. The electron temperature calculated from the slope obtained from a graph $\ln(\lambda_{ji} I_{ji}/g_j A_{ji})$ versus the energy E_j [eV] as shown in Figs. 4–6 for CuZn, Cu, and Zn respectively, a straight line has an equal slope $(-1/k_B T)$.

Table I summarizes the observed data from the Boltzmann plots with the linear fitting of the correlation coefficient (R^2) for each laser intensity. The electron temperature for the CuZn, Cn, and Zn plasma are calculated for each laser intensity, ranging from 2.1–4.8 $\times 10^8$ [W/cm^2]. The value of T_e ranges between 10847–14747 K in the case of the CuZn matrix, between 3966–5908 K for the Cu matrix, and 3591–2954 K for the Zn matrix, see Table I. However, in Fig. 7, we noticed that the electron temperature grew with laser intensity in the CuZn matrix, which agrees with the previous study [12].

In contrast, the electron temperature drops with increasing laser intensity for the Cu and Zn matrix. As the plasma approaches maximum expansion

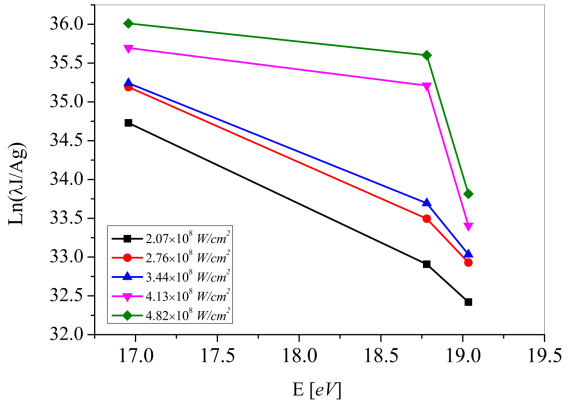

Fig. 4. The Boltzmann plots measured for the CuZn plasma at different laser irradiance.

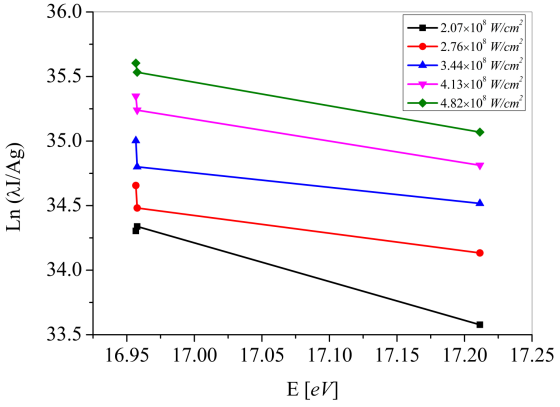

Fig. 5. Description as in Fig. 4, but for Cu plasma.

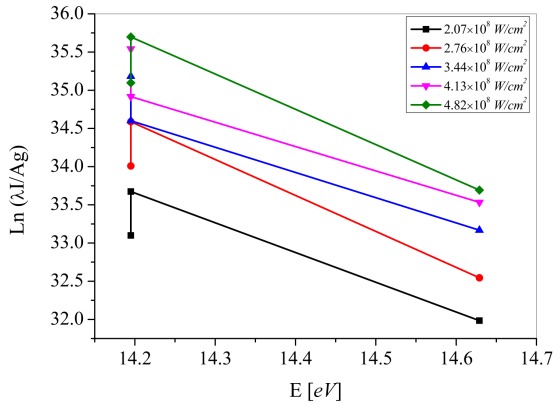

Fig. 6. Description as in Fig. 4, but for Zn plasma.

TABLE II

The electron density at different laser intensity.

Laser intensity $\times 10^8$ [W/cm^2]	CuZn matrix		Cu matrix		Zn matrix	
	FWHM [nm]	$n_e \times 10^{18}$ [cm^{-3}]	FWHM [nm]	$n_e \times 10^{18}$ [cm^{-3}]	FWHM [nm]	$n_e \times 10^{18}$ [cm^{-3}]
2.07	1.6	1.2	1.2	0.90	2.0	1.5
2.76	2.0	1.5	1.8	1.35	2.2	1.7
3.44	2.5	1.9	2.1	1.58	2.7	2
4.13	3.8	2.9	2.5	1.88	3.0	2.3
4.82	4.0	3	3.0	2.25	4.0	3

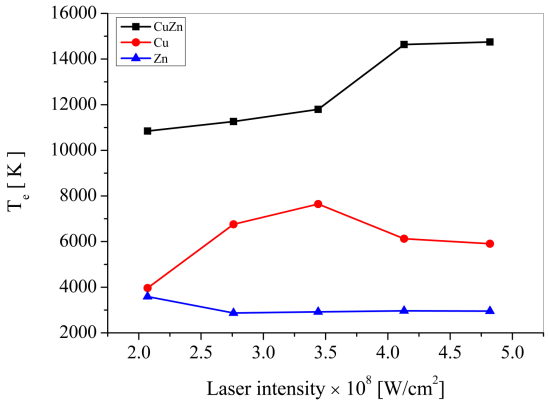

Fig. 7. The electron temperature of CuZn, Cu, and Zn matrix at different laser intensity.

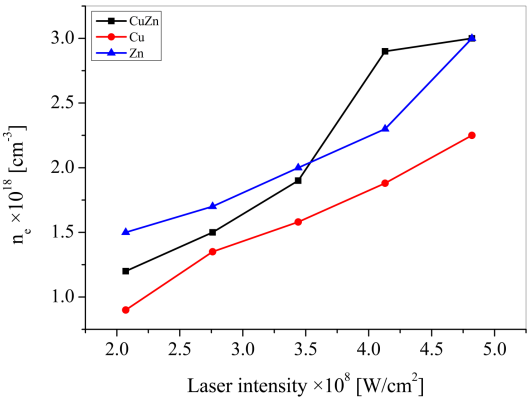

Fig. 8. The electron density of CuZn, Cu, and Zn plasma at different laser intensity.

velocities, the thermal energy is rapidly converted to kinetic energy, causing the plasma temperature to drop. This result agrees with Qindeel et al. [13]. In the LIPS technique, the fluctuation of electron temperature and the electron density is due to the matrix effect and interference of the prevalent atmospheric environment with the generated plasma. In some cases, the gas above the target surface can absorb significant laser energy (i.e., plasma shielding) [14].

3.2.2. Electron density

The emission spectra lines of the laser-generated CuZn, Cu, and Zn plasma appear as broadened lines. Collisions of the emitted atom with charged particles cause the Stark line broadening, which is the principal mechanism affecting these emission spectra. Thus, the electron density can be estimated depending on the spectral line widths through the following relation [15]

$$n_e = \left(\frac{\lambda_{FWHM}}{2w}\right) \times 10^{16}, \tag{2}$$

where n_e is the electron density [cm^{-3}], λ_{FWHM} refers to the Stark full-width at half-maximum (FHWM), and w is the electron impact parameter. The electron density is estimated from the isolated spectral lines of Cu II at 625.7 nm and Cu I at 578.2 nm emitted from CuZn and Cu plasma, respectively, whereas in the case of Zn plasma — from Zn I at 647.9 nm, for various laser intensity. The electrons density ranged from 1.2 to 3×10^{18} cm^{-3}, from 0.90 to 2.25×10^{18} cm^{-3}, and from 1.5 to 3×10^{18} cm^{-3} for CuZn, Cu, and Zn plasma, respectively, see Table II.

Figure 8 shows that the electron density increases as the laser intensity increases. The saturation/slow variation of n_e and T_e was seen in the results. The behavior observed is related to the plasma shielding effect, i.e., plasma reflection of laser light. Since the experiment is conducted atthe atmospheric pressure, the ionization process is limited by the plasma shielding effect of air, reducing the efficiency of the available laser intensity for mass ablation. In this study, the laser frequency ($\nu = c/L_\lambda$) is 5.6×10^{14} Hz for visible light (532 nm), whereas the plasma frequency is $\omega_p = 8.9 \times 10^3 n_e^{0.5}$ [12]. The electron density is $n_e = 10^{18}$ cm^{-3}, hence, $\omega_p \approx 10^{12}$ Hz is less than the laser frequency $\omega_p \approx 10^{14}$ Hz. The plasma frequency appears lower than the laser frequency. It means that the loss of energy due to Nd:YAG laser reflection on the CuZn, Cu, and Zn plasma surface is insignificant.

4. Conclusions

The laser intensity and matrix effect on the CuZn, Cu, and Zn matrix plasma parameters have been studied. The Cu and Zn plasma emission lines differ

from the CuZn plasma emission lines which is attributed to differences in thermal and optical properties of CuZn, Cu, and Zn matrix. The electron temperature of CuZn plasma increased with rising laser intensity. In contrast, no linear change in the electron temperature with the laser intensity occurs for Cu and Zn plasma. Different behavior of electron temperature is due to the matrix effect. The broadening of spectral lines appears with increased laser intensity, and this broadening is related to electron density.

Acknowledgments

The author would like to thank the supports of the Department of Physics, College of Science, Mustansiriyah University (uomustansiriyah.edu.iq) as well as the Plasma Physics Laboratory of the Department of Physics, College of Science, University of Baghdad, Iraq.

References

[1] D. Fernandes Andrade, E.R. Pereira-Filho, D. Amarasiriwardena, *Appl. Spectrosc. Rev.* **56**, 98 (2021).

[2] H. Sattar, L. Sun, M. Imran, R. Hai, D. Wu, H. Ding, *Plasma Sci. Technol.* **21**, 034019 (2019).

[3] T. Takahashi, B. Thornton, *Spectrochim. Acta B* **138**, 31 (2017).

[4] A.M. Popov, S.M. Zaytsev, I.V. Seliverstova, A.S. Zakuskin, T.A. Labutin, *Spectrochim. Acta B* **148**, 205 (2018).

[5] S. Zhang, M. He, Z. Yin, E. Zhu, W. Hang, B. Huang, *J. Anal. At. Spectrom.* **31**, 358 (2016).

[6] M.A. Al-Eshaikh, *J. Appl. Spectrosc.* **84**, 725 (2017).

[7] NIST, Atomic Spectra Database.

[8] W. Wang, L. Sun, P. Zhang, T. Chen, L. Zheng, L. Qi, *J. Anal. At. Spectrom.* **36**, 1977 (2021).

[9] D.V. Babos, A. Cruz-Conesa, E.R. Pereira-Filho, J.M. Anzano, *J. Hazard. Mater.* **399**, 122831 (2020).

[10] J. Wang, X. Li, C. Wang, L. Zhang, X. Li, *Optik* **166**, 199 (2018).

[11] M.M. ElFaham, M. Okil, A.M. Mostafa, *Opt. Laser Technol.* **108**, 634 (2018).

[12] T.K. Hamad, A.S. Jasim, H.T. Salloom, *Opt. Spectrosc.* **127**, 153 (2019).

[13] R. Qindeel, M.S. Dimitrijević, N.M. Shaikh, N. Bidin, Y.M. Daud, *Eur. Phys. J. Appl. Phys.* **50**, 30701 (2010).

[14] A.N. Kadachi, M.A. Al-Eshaikh, *Spectrosc. Lett.* **48**, 403 (2015).

[15] M. Fikry, W. Tawfik, M.M. Omar, *Opt. Quantum Electron.* **52**, 249 (2020).